JACS
JOURNAL OF THE AMERICAN CHEMICAL SOCIETY

Article

pubs.acs.org/JACS

An Ionic Liquid Dependent Mechanism for Base Catalyzed β-Elimination Reactions from QM/MM Simulations

Caley Allen, Somisetti V. Sambasivarao, and Orlando Acevedo*

Department of Chemistry and Biochemistry, Auburn University, Auburn, Alabama 36849, United States

Supporting Information

ABSTRACT: Ionic liquids have been proposed to induce a mechanistic change in the reaction pathway for the fundamentally important base-induced β-elimination class compared to conventional solvents. The role of the reaction medium in the elimination of 1,1,1-tribromo-2,2-bis(3,4-dimethoxyphenyl)ethane via two bases, piperidine and pyrrolidine, has been computationally investigated using methanol and the ionic liquids 1-butyl-3-methylimidazolium tetrafluoroborate and hexafluorophosphate [BMIM][BF_4] and [BMIM][PF_6], respectively. QM/MM Monte Carlo simulations utilizing free-energy perturbation theory found the ionic liquids did produce a reaction pathway change from an E1cB-like mechanism in methanol to a pure E2 route that is consistent with experimental observations. The origin of the ionic liquid effect has been found as: (1) a combination of favorable electrostatic interactions, for example, bromine-imidazolium ion, and (2) π−π interactions that enhance the coplanarity between aromatic rings maximizing the electronic effects exerted on the reaction route. Solute−solvent interaction energies have been analyzed and show that liquid clathrate solvation of the transition state is primarily responsible for the observed mechanistic changes. This work provides the first theoretical evidence of an ionic liquid dependent mechanism and elucidates the interplay between sterics and electrostatics crucial to understanding the effect of these unique solvents upon chemical reactions.

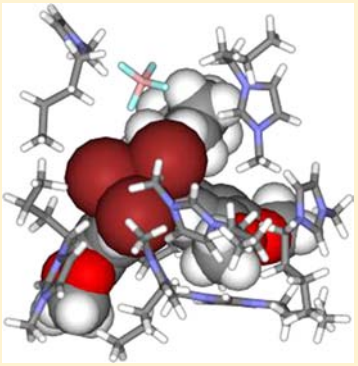

INTRODUCTION

Room temperature ionic liquids are an exciting class of solvents that have the potential to accelerate and control a vast range of reactions.[1] Ionic liquids are generally defined as a material containing only ionic species with a melting point below 100 °C.[1,2] These "designer" solvents are typically composed of a low symmetry organic cation, such as the 1-alkyl-3-methylimidazolium [RMIM] cation (R = M (methyl), E (ethyl), B (butyl), H (hexyl), and O (octyl)), and a weakly coordinating inorganic or organic anion with a diffuse negative charge like hexafluorophosphate [PF_6] or tetrafluoroborate [BF_4].[3,4] Ion components can be fine-tuned through different functional groups to enhance the degree of localized structuring in the liquid phase, which distinguishes ionic liquids from molecular solvents and solutions containing dissociated ions.[4] The use of ionic liquids as a reaction medium for chemical reactions has dramatically increased in recent years, due in large part to numerous reported advances in catalysis,[5] separation science,[6] and organic synthesis[7] when employing the unique solvents. For example, the Diels−Alder reaction, paradigm in organic synthesis, highlights the advantages provided by ionic liquids as the reaction between cyclopentadiene and methyl acrylate in 1-ethyl-3-methylimidazolium tetrachloroaluminate and heptachlorodialuminate [EMIM][$AlCl_4$] and [EMIM][Al_2Cl_7], respectively, has been reported to react with rates over 200 times faster and *endo* selectivity 10 times greater than commonly used reaction conditions.[8] Our QM/MM investigation of the same Diels−Alder reaction in the chloroaluminate ionic liquids emphasized the importance of intermolecular interactions on the rate of reaction with excellent $\Delta\Delta G^{\ddagger}$ agreement reported between the solvents.[9,10] Another example of recent success utilizing our QM/MM method was the Kemp elimination ring-opening of benzisoxazole in 1-butyl-3-methylimidazolium hexafluorophosphate [BMIM][PF_6] using piperidine as the base.[11] Whereas multiple organic systems have been reported experimentally,[1] theoretical calculations have only begun to elucidate the microscopic details on how ionic liquids operate upon chemical reactions.

Of current interest is the effect of ionic liquids upon the dehydrobromination reaction reported by D'Anna et al. for the β-elimination of 1,1,1-tribromo-2,2-bis(3,4-dimethoxyphenyl)-ethane by cyclic amines (Scheme 1).[12] An interesting hypothesis was put forth that a change in the reaction mechanism occurs from an irreversible E1cb route in methanol[13] to an E2 in the ionic liquids. The E2 mechanism is a one-stage process in which the base attacks the β-hydrogen

Scheme 1. β-Elimination Reaction of 1,1,1-Tribromo-2,2-bis(3,4-dimethoxyphenyl)ethane

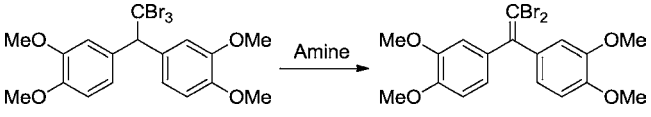

Received: October 5, 2012
Published: December 31, 2012

dx.doi.org/10.1021/ja3098614 | J. Am. Chem. Soc. 2013, 135, 1065−1072

and abstracts it with a concomitant cleavage of the α-C−Br bond; in the E1cb process, the removal of the β-hydrogen is rate limiting and generally reversible, and can be detected by isotopic exchange studies (Scheme 2).[14] Despite the obvious

Scheme 2. General E1cb and E2 Elimination Mechanisms

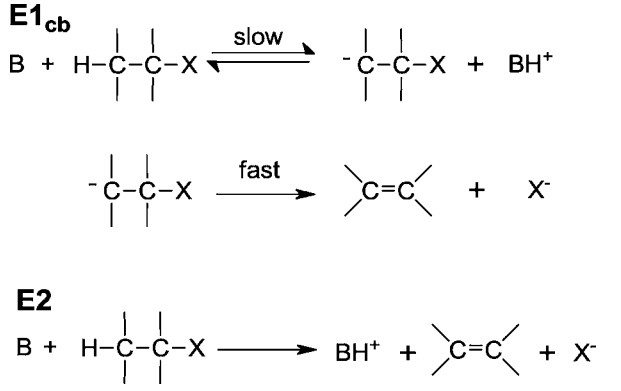

differences in the mechanisms, experimentally distinguishing between the irreversible E1cb and E2 mechanisms for dehydrohalogenation reactions can be notoriously difficult.[13,15−18] The present work applied mixed quantum and molecular mechanical (QM/MM) calculations utilizing Monte Carlo sampling and free-energy perturbation theory (MC/FEP) to the β-eliminations in methanol, [BMIM][BF_4], and [BMIM][PF_6] to investigate the proposed mechanism change and its origins. Two secondary cyclic amine bases, pyrrolidine and piperidine, were studied as intriguingly no primary or tertiary amines were found to experimentally induce eliminations. The QM/MM simulations with explicit solvent representation can provide the medium-dependence of the activation barriers and atomic-level structural detail for characterization of the nature of the ionic liquids. Comparisons are made to density functional theory (DFT) calculations using an implicit continuum model to simulate conventional solvent effects. The results presented provide new insights as to the ionic liquid effects on the reaction pathway and help clarify experimental observations.

■ COMPUTATIONAL METHODS

QM/MM calculations were carried out on 1,1,1-tribromo-2,2-bis(3,4-dimethoxyphenyl)ethane with piperidine and pyrrolidine in [BMIM]-[BF_4], [BMIM][PF_6], and methanol. The solutes were treated with the PDDG/PM3 semiempirical QM method.[19] PDDG/PM3 has given excellent results for a wide variety of organic and enzymatic reactions in the solution-phase.[20−23] Potentials of mean force (PMF) calculations coupled to Metropolis Monte Carlo (MC) statistical mechanics were used to build a free-energy profile for the β-elimination reactions at 25 °C and 1 atm. The starting geometries for the solutes were determined by executing a MC conformational search that resulted in up to 100 unique structures. The top 10 most favorable MC structures were then recomputed using full DFT geometry optimizations and the resultant lowest energy structure was used as the starting geometry for the QM/MM calculations. The solvent molecules were represented explicitly using our custom ionic liquid OPLS-AA force field[11] and the united-atom OPLS force field for methanol.[24] The current QM/MM methodology allows simulations of reactions in solution on-the-fly with full sampling and polarization of the solutes by the environment.[25] The systems consisted of the reactants plus 395 solvent molecules for methanol or 188 ion pairs for the ionic liquids. The boxes are periodic and tetragonal with c/a = 1.5 where a is 26.7, 34.3, and 35.5 Å for methanol, [BMIM][BF_4], and [BMIM][PF_6], respectively, with long-range electrostatic interactions handled with Ewald summations. The ionic liquid boxes were thoroughly equilibrated by raising the temperature to 1000 °C and carrying out 10 million configurations in the NVT ensemble. The simulations were then equilibrated at 25 °C for 100−200 million MC steps in the NPT ensemble. The heating/NVT and equilibration/NPT simulations on each ionic liquid system were repeated sequentially an average of 4−6 times until the energy and volume of the system no longer changed. Solutes were inserted with the appropriate solute geometry corresponding to each free energy perturbation (FEP) window and re-equilibrated for minimally 100 million MC configurations. The computation of the QM energy and atomic charges was performed for each attempted move of the solute, which occurred every 100 configurations. For electrostatic contributions to the solute−solvent energy, CM3 charges[26] were obtained for the solute and scaled by 1.14 to reflect the polarization in a condensed-phase environment.[27] In addition, Lennard-Jones interactions between solute and solvent atoms were taken into account using OPLS parameters. This combination is appropriate for a PM3-based method as it minimizes errors in computed free energies of hydration.[28]

The simulations were performed with the BOSS program.[29] All cations were fully flexible; that is, all bond stretching, angle bending, and torsional motions were sampled. Anions were simulated as rigid molecules. The use of rigid anions in OPLS-AA has been shown to provide an accurate representation of ionic liquid physical properties, including use as a reaction medium for computed QM/MM Diels−Alder[9] and Kemp elimination[11] reaction studies. Solute−solvent and solvent−solvent intermolecular cutoff distances of 12 Å were employed for the tail carbon atom of each side chain (methyl and alkyl), a midpoint carbon on the alkyl chain, and the ring carbon between both nitrogens for imidazolium. Center atoms, for example, B in BF_4^- and P in PF_6^-, were used for the anions. If any distance is within the cutoff, the entire solvent−solvent interaction was included. Adjustments to the allowed ranges for rotations, translations, and dihedral angle movements led to overall acceptance rates of about 30% for new configurations. The ranges for bond stretching and angle bending were set automatically by the BOSS program on the basis of force constants and temperature.

Free energy maps were computed by using a distance, $R_{NH} - R_{HC}$, for the proton transfer between the nitrogen on piperidine/pyrrolidine and the reacting hydrogen on the solute; $R_{NH} + R_{HC}$ was kept constant at 2.85 Å. The fixed distance of 2.85 Å was determined to be appropriate from our recent work[11,22] and additional test calculations. Our fifth-order polynomial quadrature method was used to provide a 7-fold improvement in speed over traditional potentials of mean force (PMF) methods.[22] A second perturbation was necessary, R_{CBr}, which entailed breaking of the C−Br bond. Combining the $R_{NH} - R_{HC}$ PMF which runs along one reaction coordinate with the R_{CBr} PMF in a second direction produced a two-dimensional (2D) PMF. The resultant free-energy map was used to identify minima and the transition state present in the reaction. The breaking of the C−Br bond was split into increments of 0.025 Å. Each PMF calculation required extensive reorganization of the solvent for the ionic liquid, requiring up to 125 million configurations of equilibration followed by 10 million MC steps of averaging per FEP window; in methanol, 2 and 5 million steps of equilibration and averaging, respectively, sufficed for each reaction. Every solution-phase MC/FEP calculation required over 100 million single point QM calculations per free-energy map in the ionic liquids, demonstrating the need for highly efficient QM methods.

The M06-2X density functional method[30] and 6-31+G(d,p) basis set were also used to optimize geometries in vacuum, methanol, and water using Gaussian 09.[31] The effect of solvent was explored by full DFT geometry optimizations using the conductor-like polarizable continuum model (CPCM) with the UFF cavity.[32] Frequency calculations were performed in order to verify all stationary points as minima for ground states or as saddle points for transition structures. All calculations were run on a Linux cluster at Auburn University and on computers located at the Alabama Supercomputer Center.

RESULTS AND DISCUSSION

Energetics. The QM/MM/MC calculations for the β-elimination of 1,1,1-tribromo-2,2-bis(3,4-dimethoxyphenyl)-ethane in methanol gave computed activation barriers $\Delta G^{\ddagger}$ of 36.5 and 34.6 kcal/mol when using piperidine and pyrrolidine, respectively. The $\Delta\Delta G^{\ddagger}$ values between the secondary amines are consistent with experimental trends, where pyrrolidine is reported to react faster than piperidine based on measurements of second order rate constants.[12] Interestingly, the ring dimension rather than nitrogen basicity appears to control the rate, where the flexibility of the ring is thought to play a major role.[12] Error ranges in the computed free-energy values have been estimated from fluctuations in the ΔG values for each FEP window using the batch means procedure with batch sizes of 0.5 million configurations; computed errors in the free energies imply overall uncertainties in the $\Delta G^{\ddagger}$ of ca. 0.5 kcal/mol. Table 1 gives a summary of the activation energies and reacting geometries for the reactions in methanol and the ionic liquids. Errors in the free energies and geometries for the ionic liquids result in overall uncertainties of approximately 1.5 kcal/mol and ±0.1 Å.

Table 1. Free Energy of Activation, $\Delta G^{\ddagger}$ (kcal/mol) and Transition Structure Geometries (Å) at 25 °C for the β-Elimination of 1,1,1-Tribromo-2,2-bis(3,4-dimethoxyphenyl)ethane in Ionic Liquid from QM/MM/MC Calculations[a]

	$\Delta G^{\ddagger}$ (calc)	R(C−Br)	$\Delta G^{\ddagger}$ (exptl)[b]
piperidine			
methanol	36.5	2.43	-
[BMIM][BF_4]	34.8	2.68	24.2
[BMIM][PF_6]	29.2	2.58	23.9
pyrrolidine			
methanol	34.6	2.33	-
[BMIM][BF_4]	36.3	2.63	22.7
[BMIM][PF_6]	28.9	2.60	-

[a]PDDG/PM3 and MC/FEP. [b]Ref 12.

The calculated $\Delta G^{\ddagger}$ overestimation is a systematic error common in many organic reactions when employing a semiempirical method.[33] Dewar also reported mixed energetic agreement with experiment when employing the AM1 method on elimination reactions, but the analogous trends provided excellent results in differentiating between E2, E1cb-like, and SN2 mechanisms.[34] In addition, COSMO-AM1 and experimental values of the free activation enthalpy on a set of elimination reactions in water showed large discrepancies; however, reactivity aspects were correctly predicted.[35] It is important to note that the overestimation of the absolute $\Delta G^{\ddagger}$ value using semiempirical QM/MM methods is not limited to the dehydrobromination reaction as similar findings have been reported for multiple Diels−Alder reactions,[9,36] ene reactions,[23] Claisen rearrangements,[21] and methyl transfer reactions.[37] Conceivably, a straightforward reparameterization of the PDDG/PM3 Hamiltonian by scaling the energies from points along the reaction coordinate could provide accurate $\Delta G^{\ddagger}$ values; however, the physical reasons for determining structures would be absolutely the same as the original Hamiltonian. Consequently, there is no difference in leaving the Hamiltonian in its original form or in scaling the energies when one considers the relative solvent effects.

E1cb versus E2 Mechanism. A representative free energy map from the QM/MM/MC calculations in methanol (Figure 1) predicts a concerted E2 transition structure with a large amount of proton transfer characteristic of an E1cb-like mechanism, but not the irreversible stepwise E1cb route proposed in recent publications[12,13,16] as no carbanion intermediate was located. The differences in the results may be rationalized through the disparities in base strengths used, where the base reported MeO^- is an extremely strong base relative to the cyclic amines and could potentially accelerate proton removal but not affect the carbanion decomposition.[14] However, pyrrolidine was reported to induce elimination of the current tribromo-ethane reactant faster than a methoxide/methanol reaction despite the difference in basicity.[12] Experimental studies have proposed that the transition structure should be strikingly similar for E1cb and E2 mechanisms.[16,17] For example, Gandler and Jencks speculated in 1982 about a theoretical potential energy surface for the elimination reactions of (2-arylethyl)quinulidinium ions where the transition state for the E1cb mechanism converts into an E2 mechanism as a substituent change to a β-phenyl group caused the carbanion to become less stable and cease to exist (Figure 2).[18] In addition to the β-phenyl groups present in the current reaction, Br as a leaving group generally tends to favor the E2 mechanism, as does the use of a moderate-strength base, such as the cyclic amines piperidine and pyrrolidine, in polar solvents.[38] It should be noted that the banding observed in Figure 1 is a consequence of using of 0.05 Å increments in the FEP calculations. To locate the critical points more precisely, the regions surrounding the free-energy minima and maxima from the initial maps in all solvents were explored using final increments of 0.025 Å with increased sampling. This provided the refined results in the energetics and geometries for the β-elimination reactions summarized in Table 1.

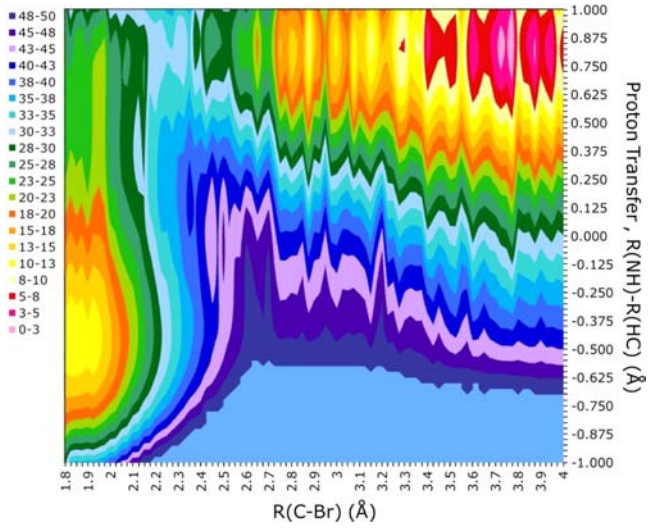

Figure 1. Free energy map (kcal/mol) computed for the β-elimination of 1,1,1-tribromo-2,2-bis(3,4-dimethoxyphenyl)ethane with piperidine in methanol from QM/MM/MC simulations. Energy values truncated after 50 kcal/mol for clarity.

As another point of reference, DFT calculations were carried out using the M06-2X/6-31G+(d,p) method in vacuum and in solution (methanol and water) by using the CPCM continuum solvent method (Table 2). In the gas-phase, the DFT method predicted a traditional E2 mechanism, where the C−Br

dx.doi.org/10.1021/ja3098614 | J. Am. Chem. Soc. 2013, 135, 1065−1072

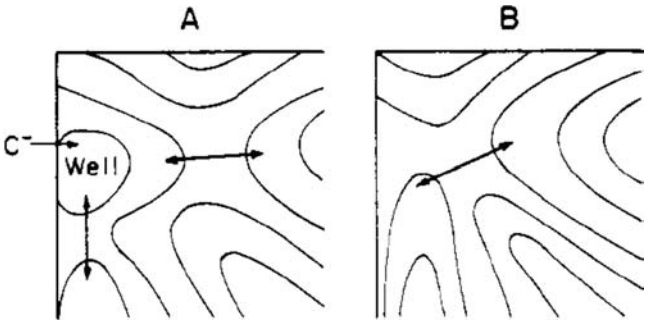

Figure 2. Speculative reactive coordinate contour diagram proposed by Gandler and Jencks[18] to illustrate the transition from an E1cb mechanism with a carbanion intermediate (A) to a concerted E2 mechanism when the carbanion no longer exists (B).

Table 2. Free Energy of Activation, $\Delta G^{\ddagger}$ (kcal/mol), and Transition Structure Geometries (Å) at 25 °C for the β-Elimination of 1,1,1-Tribromo-2,2-bis(3,4-dimethoxyphenyl)ethane from M06-2X/6-31+G(d,p)/CPCM

	$\Delta G^{\ddagger}$ (calc)	R(C−Br)
	piperidine	
gas	27.7	2.31
methanol	19.9	2.16
water	20.2	2.16
	pyrrolidine	
gas	28.7	2.35
methanol	19.0	2.15
water	19.2	2.15

making/breaking bond distance is 2.31−2.35 Å and is moving in concert with the proton transfer when visualizing the 'imaginary frequency,'[39] for example, −150.85 cm^{-1} for piperidine. In contrast, the single 'imaginary frequency' of −1166.51 or −1181.18 cm^{-1} for the reaction with piperidine in methanol and water, respectively, showed the proton transfer motion occurring with stationary, but extended C−Br distances of 2.16 and 2.15 Å (Figure 3 and Table 2) compared to the equilibrium distance of ca. 1.94 Å. The transition state C−Br distance is predicted to be earlier in solution than gas. The DFT calculations are in agreement with the QM/MM/MC simulations in methanol suggesting an E1cb-like mechanism, that is, E2 with a significant amount of E1cb character, in accord with experiment[13] and with previous studies of borderline cases between E2 and E1cb mechanisms.[40]

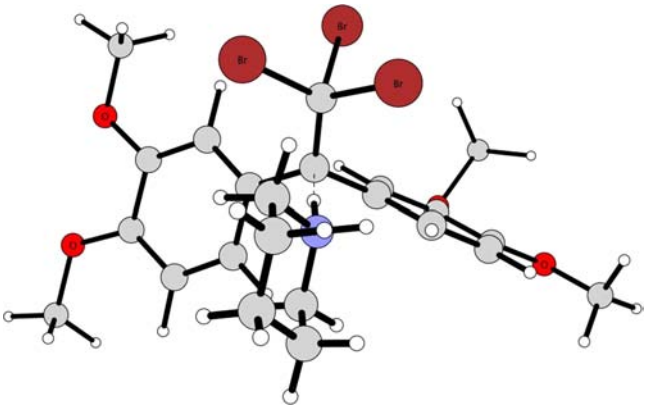

Figure 3. Illustration of the optimized transition structure for the β-elimination of 1,1,1-tribromo-2,2-bis(3,4-dimethoxyphenyl)ethane with piperidine in methanol from the M06-2X/6-31+G(d,p)/CPCM calculation.

Charges. The scaled CM3 charges computed for the β-elimination in each solvent can also be used to differentiate between mechanisms. For example, a greater concentration of anionic charge in the antiperiplanar reacting Br at the transition state would be more indicative of a traditional E2 reaction pathway than a distributed negative charge, spread among the Br and ethane carbon atoms, expected from an irreversible E1cb carbanion. In the QM/MM/MC calculations, the leaving Br in the β-elimination transition structures in [BMIM][BF_4] and [BMIM][PF_6] have computed partial charges of −0.94 e compared to −0.54 e in methanol. Figure 4 gives selected atomic charges for the transition state with piperidine in the ionic liquids and methanol; Figure S1 in the Supporting Information gives the charges for the pyrrolidine system. In addition, the partial charges on the ethane carbon responsible for proton transfer are more positive in the ionic liquids than in methanol, that is, −0.23 and −0.16 e in [BMIM][BF_4] and [BMIM][PF_6], respectively, compared to −0.45 e in CH_3OH. The more developed Br charge in the ionic liquids in concert with the extensive proton transfer at the transition state is more consistent with a pure E2 mechanism. The greater concentration of negative charge on the solute at the transition structure in methanol is more indicative of a reaction with considerable E1cb character. Consistent with the charges, the QM/MM/MC calculations for the dehydrobromination in the [BMIM][BF_4] and [BMIM][PF_6] ionic liquids predicted the C−Br bond cleavage at the transition structure to be noticeably longer, ca. 2.6−2.7 Å, compared to the distances of 2.3−2.4 Å in methanol for piperidine and pyrrolidine (Table 1). The charges on the piperidine N and reacting H are essentially the same in all solvents suggesting that solvation of the leaving group may be primarily responsible for the difference in mechanism.

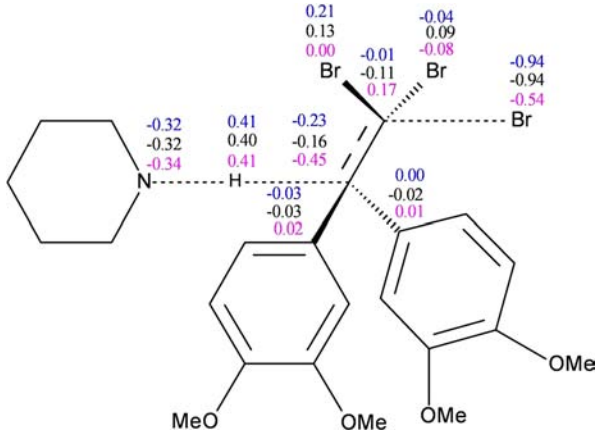

Figure 4. Selected atomic charges (e units) for the transition structure in [BMIM][BF_4] (blue), [BMIM][PF_6] (black), and methanol (pink) for the β-elimination of 1,1,1-tribromo-2,2-bis(3,4-dimethoxyphenyl)-ethane with piperidine from the QM/MM/MC calculations.

Solute−Solvent Interactions. To elucidate the differences between the ionic liquids and methanol, the interaction energies for the solvents were quantified by analyzing the solute−solvent energy pair distributions from QM/MM/MC calculations in the representative FEP windows near the

dx.doi.org/10.1021/ja3098614 | J. Am. Chem. Soc. 2013, 135, 1065−1072

reactants and transition state. The distributions record the average number of ions in the ionic liquids or molecules for methanol that interact with the reacting system and their corresponding energies. Highly favorable electrostatic interactions between solute and solvent components are reflected in the left-most region with energies more attractive than ca. −5 kcal/mol (Figure 5 and Figure S2 in the Supporting Information). The large band near 0 kcal/mol arises from the many ions in outer shells.

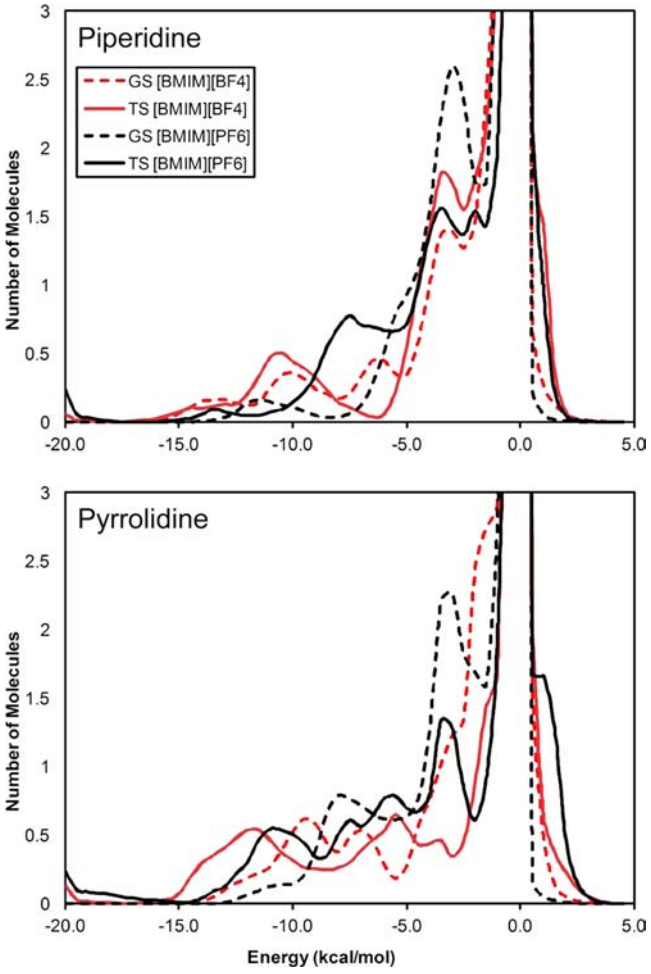

Figure 5. Solute−solvent energy pair distributions for β-elimination of 1,1,1-tribromo-2,2-bis(3,4-dimethoxyphenyl)ethane with piperidine (top) and pyrrolidine (bottom) for the reactants (dashed line) and transition state (solid line) in [BMIM][BF_4] and [BMIM][PF_6] at 25 °C. The ordinate records the number of solvent molecules that interact with the solutes and their interaction energy on the abscissa. Units for ordinate are number of molecules per kcal/mol.

The β-elimination reactions with piperidine and pyrrolidine have weaker energy distributions for the reactants when compared to the transition state in both ionic liquids and in methanol (Figures 5 and S2). Integration of the distributions from −10.0 to −5.0 (or −3.5) kcal/mol confirms the more favorable interactions for the transition states (Table 3). Specifically, the number of solute−solvent interactions increases by 1−3 ions in going from the reactants to transition state in the ionic liquids. In addition, there is a shift in the average strength of the most favorable interactions to lower energy particularly for pyrrolidine, which could explain the enhanced rate of reaction reported versus piperidine.[12]

Table 3. Solute−Solvent Energy Pair Distributions for the β-Elimination of 1,1,1-Tribromo-2,2-bis(3,4-dimethoxyphenyl)ethane for the Reactant (GS) and Transition Structure (TS) in [BMIM][BF_4], [BMIM][PF_6], and Methanol Integrated to −5.0 kcal/mol (and −3.5 kcal/mol in parentheses)[a]

	Piperidine		Pyrrolidine	
	GS	TS	GS	TS
[BMIM][BF_4]	5.1 (8.0)	4.9 (9.2)	6.1 (8.5)	8.2 (9.6)
[BMIM][PF_6]	3.7 (8.6)	7.1 (11.1)	6.7 (10.9)	9.3 (12.1)
methanol	1.3 (2.9)	6.4 (9.2)	2.5 (4.8)	4.7 (8.6)

[a]From Figures 5 and S2.

The exact nature of these most favorable solute-ion interactions is of obviously relevant interest. In both reactions, a shift in the average strength of the most favorable interactions to a lower energy in the transition state is consistent with the stabilization of the emerging charge at the reacting Br. Figure 6

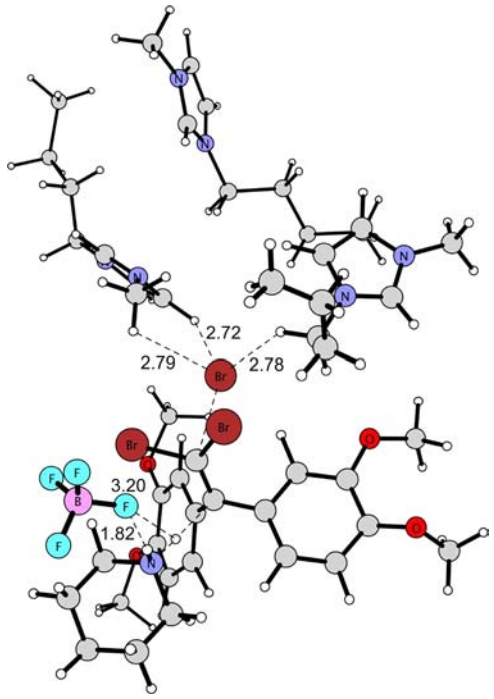

Figure 6. Typical snapshot of a transition state for the β-elimination with piperidine in [BMIM][BF_4]. The distances (in Å) are average values over the final 10 million configurations of QM/MM/MC simulations. Only nearby ions retained for clarity.

shows a snapshot of the piperidine-based β-elimination transition structure in [BMIM][BF_4] with nearby ions retained from the QM/MM/MC simulations. The emerging Br anion is stabilized by two BMIM cations forming hydrogen bonds with the more sterically exposed hydrogens on carbons at the 4 and 5 positions and the side chain hydrogens, rather than the most acidic imidazolium proton at the 2 position (pK_a of ca. 21−23).[41] The BMIM cations are forming a cage-like structure to favorably interact with the Br anion and β-phenyl substituents (Figure 7), which agrees with experimental reports of liquid clathrate formation in 1-alkyl-3-methylimdazolium-based ionic liquids with aromatic compounds.[42] In addition, the proton transfer is facilitated by favorable electrostatic interactions of the emerging positive charge on the base with a BF_4 anion

dx.doi.org/10.1021/ja3098614 | J. Am. Chem. Soc. 2013, 135, 1065−1072

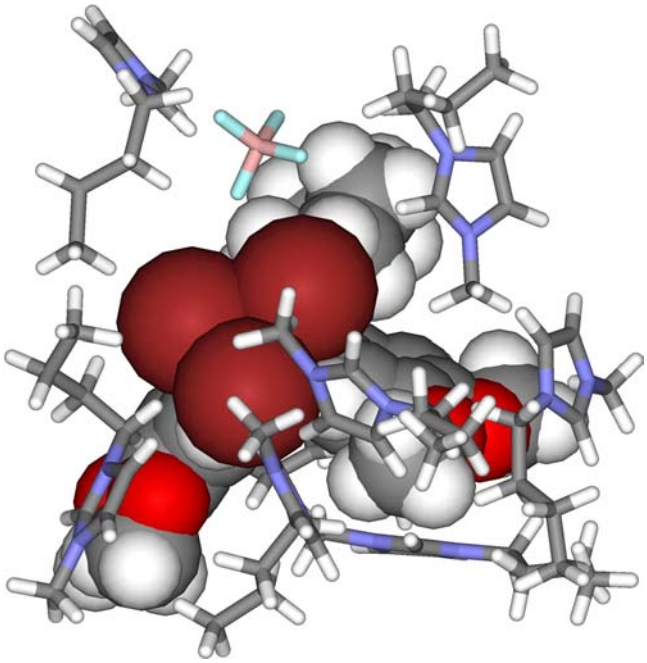

Figure 7. Illustration of the encapsulation of the β-elimination solute with piperidine transition state (given as a CPK space-filling model) by nearby ions from [BMIM][BF_4] (shown as sticks).

(Figure 6). While the averaged polarity of methanol and [BMIM][BF_4] is similar,[43] the experimentally measured dipolarity/polarizability (π^*) values for [BMIM][BF_4] and [BMIM][PF_6] of 1.047 and 1.032, respectively, are significantly higher than that of 0.73 for methanol.[44] This is consistent with more the favorable specific interactions toward the E2 mechanism by the ionic liquids as compared to methanol.

The ground state, represented by a reactant complex between the base and the tribromo-ethane, has computed interactions between the ions and the reactants at greater distances than at the transition structure. For example, in the piperidine reaction in [BMIM][BF_4], the cation interacts with the emerging Br anion with multiple interacting distances as short as 2.7 Å at the transition state, whereas the closest interaction at the ground state is 3.0 Å and it occurs with the less acidic hydrogen atoms bonded to the methyl side chain. The results are similar for the [PF_6]-based reactions. Detailed hydrogen bonding distances between the ionic liquids ions and the piperidine- and pyrrolidine-based β-eliminations at the transition and ground states are given in the Supporting Information. The structural configuration of the methanol molecules with the transition and ground states are also given in the Supporting Information and support the computed reduced solute−solvent interaction energies as compared to the ionic liquids.

Aromatic Ring Orientations. A snapshot of the transition state for the elimination reaction using pyrrolidine in [BMIM][PF_6] is given in Figure 8 and gives a good representation of the geometry orientation for the reactions in both ionic liquids (Table 4). The ionic liquid structures have the aromatic rings generally coplanar at the transition state. For example, torsion angles of −146.4 and 134.5° between the two carbons on the aromatic ring and the two carbons on the ethane, defined as Φ_1 and Φ_2 = C1−C2−C3−C4 in Figure 8, for piperidine in [BMIM][BF_4] are a dramatic contrast from the values of −162.6 and 87.1° predicted from DFT (Figure 3)

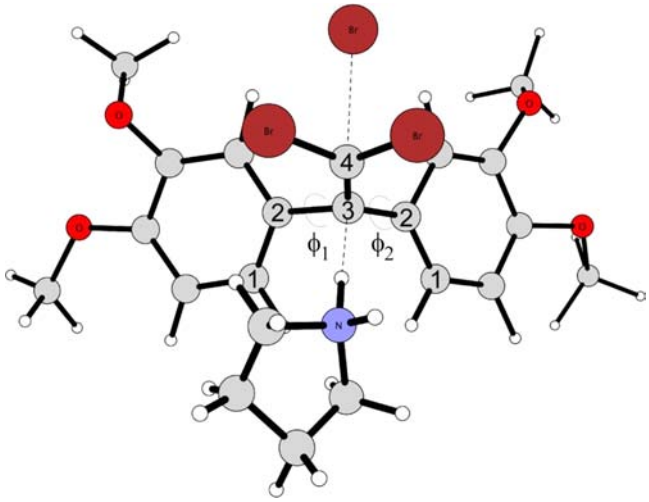

Figure 8. Snapshot of a transition state for the β-elimination of 1,1,1-tribromo-2,2-bis(3,4-dimethoxyphenyl)ethane with pyrrolidine in [BMIM][PF_6] from the QM/MM/MC calculations. Φ = C1−C2−C3−C4.

Table 4. Dihedral Angles Φ_1/Φ_2 (degrees) for the Transition Structure at 25 °C for the β-Elimination of 1,1,1-Tribromo-2,2-bis(3,4-dimethoxyphenyl)ethane[a]

	QM/MM[b]	DFT[c]
	piperidine	
[BMIM][BF_4]	−146.4/134.5	-
[BMIM][PF_6]	−105.9/113.2	-
Methanol	−154.4/113.5	−162.6/87.1
Water	-	−162.6/87.1
Gas	-	−154.1/83.7
	pyrrolidine	
[BMIM][BF_4]	−106.4/132.7	-
[BMIM][PF_6]	−135.3/129.8	-
Methanol	−173.9/126.2	−157.8/89.1
Water	-	−157.8/89.2

[a]See Figure 8 for definitions of Φ_1 and Φ_2. [b]PDDG/PM3 and MC/FEP. Angles averaged over final 10 million configurations. [c]M06-2X/6-31+G(d,p) optimization.

or −154.4 and 113.5° from QM/MM/MC for the same reaction in methanol.

The coplanar orientation of the phenyl rings at the transition state should maximize the electronic effects exerted on the reaction route. Favorable $\pi-\pi$ interactions with the ionic liquid cation [BMIM] forces a coplanarity between aromatic rings (Figure 7 and Supporting Information Figure S3), which is consistent with previous hypotheses.[42,45] It should be noted that the OPLS-AA force field has been reported to yield excellent agreement with experiment for computed benzene dimer interaction energies and geometries in the gas and condensed phase.[46] More recently, Fu and Tian carried out molecular dynamics (MD) simulations for liquid benzene with eight potentials consisting of Lennard-Jones and Coulomb terms and recommended the OPLS-AA as the best model based agreement with high-resolution neutron diffraction data.[47] In addition, Takeuchi also reported that the OPLS-AA force field was more reliable in reproducing the structures of benzene clusters, consisting of up to 30 rings, than MP2 calculations.[48]

dx.doi.org/10.1021/ja3098614 | J. Am. Chem. Soc. 2013, 135, 1065−1072

Monitoring the average Φ_1 and Φ_2 torsions over the final 10 million configurations of the QM/MM/MC calculations suggests that the reaction spends minimally 70% of the simulation in the coplanar configuration and 30% in a t-shaped configuration. In contrast, the transition structures in methanol adopted an approximate t-shaped conformation for nearly 100% of the QM/MM/MC simulations. The aromatic rings of the reaction in water were also predicted to favor a t-shaped orientation from DFT simulations (Table 3).

CONCLUSIONS

QM/MM calculations have been carried out to determine the origin of the ionic liquid effect on a reported mechanism change for the β-elimination between 1,1,1-tribromo-2,2-bis(3,4-dimethoxyphenyl)ethane and the cyclic amines piperidine and pyrrolidine. D'Anna et al. proposed the reaction to occur via an irreversible E1cb route in methanol,[13] but as an E2 mechanism in the [BMIM][BF_4] and [BMIM][PF_6] ionic liquids.[12] Our computed free energy surfaces agree in principle with their hypothesis, with the exception that in methanol the reaction route followed an E1cb-like mechanism, that is, E2 with a significant amount of E1cb character, as no carbanion intermediate was located. Our results are consistent with previous experimental studies of borderline cases between E2 and E1cb mechanisms.[40] The E1cb-like mechanism in methanol is further verified with additional calculations using an alternative M06-2X/CPCM method. In the case of the two ionic liquids studied, [BMIM][BF_4] and [BMIM][PF_6], the simulations reproduced the full E2 mechanism as suggested. The structural configuration of the ions play a large role, as the observed mechanistic change has been computed as a combination of favorable electrostatic interactions with the leaving Br anion and $\pi-\pi$ interactions between the [BMIM] cation and β-phenyl substituents on the tribromo-ethane molecule. Specifically, the number of solute−solvent interactions are computed to increase by 1 to 3 ions in going from the reactants to transition state in the ionic liquids. There is a shift in the average strength of the most favorable interactions to lower energy, particularly for pyrrolidine, which could explain the enhanced rate of reaction reported versus piperidine.[12] In addition, the ionic liquids form a liquid clathrate structure that enforce a coplanar orientation of the β-phenyl rings at the transition state maximizing the electronic effects exerted on the reaction route.[42,45] Monitoring the average torsions over the final 10 million MC configurations of the QM/MM calculations found the phenyl rings to spend minimally 70% of the simulation in the coplanar configuration and 30% in a t-shaped configuration. In contrast, the transition structures in methanol adopted an approximate t-shaped conformation for nearly 100% of the simulation for both the QM/MM and M06-2X /CPCM methods. Deeper insight into the effect of ionic liquids upon important organic reaction types should allow researchers to exploit this understanding to predict optimal conditions for additional reactions in similar classes.

ASSOCIATED CONTENT

Supporting Information

Additional figures for charges and transition states in solution; solute−solvent energy pair distributions; hydrogen bond distances between ions/methanol and solute at the transition and ground states; DFT energies, frequencies, and coordinates of structures; and complete ref 31. This material is available free of charge via the Internet at http://pubs.acs.org.

AUTHOR INFORMATION

Corresponding Author

orlando.acevedo@auburn.edu

Notes

The authors declare no competing financial interest.

ACKNOWLEDGMENTS

Gratitude is expressed to the National Science Foundation (CHE-1149604) and the Alabama Supercomputer Center for support of this research.

REFERENCES

(1) Hallett, J. P.; Welton, T. *Chem. Rev.* **2011**, *111*, 3508−3576.
(2) (a) Weingaertner, H. *Angew. Chem., Int. Ed.* **2008**, *47*, 654−670. (b) Forsyth, S. A.; Pringle, J. M.; MacFarlane, D. R. *Aust. J. Chem.* **2004**, *57*, 113−119. (c) Welton, T. *Chem. Rev.* **1999**, *99*, 2071−2083.
(3) Bonhote, P.; Dias, A.-P.; Papageorgiou, N.; Kalyanasundaram, K.; Gratzel, M. *Inorg. Chem.* **1996**, *35*, 1168−1178.
(4) (a) Iwata, K.; Okajima, H.; Saha, S.; Hamaguchi, H. *Acc. Chem. Res.* **2007**, *40*, 1174−1181. (b) Castner, E. W.; Wishart, J. F.; Shirota, H. *Acc. Chem. Res.* **2007**, *40*, 1217−1227.
(5) (a) Pârvulescu, V. I.; Hardacre, C. *Chem. Rev.* **2007**, *107*, 2615−2665. (b) van Rantwijk, F.; Sheldon, R. A. *Chem. Rev.* **2007**, *107*, 2757−2785. (c) Welton, T. *Coord. Chem. Rev.* **2004**, *248*, 2459−2477.
(6) Han, X.; Armstrong, D. W. *Acc. Chem. Res.* **2007**, *40*, 1079−1086.
(7) (a) Haumann, M.; Riisager, A. *Chem. Rev.* **2008**, *108*, 1474−1497. (b) Zhang, Z. C. *Adv. Catal.* **2006**, *49*, 153−237.
(8) (a) Lee, C. *Tetrahedron Lett.* **1999**, *40*, 2461−2464. (b) Fischera, T.; Sethia, A.; Weltona, T.; Woolf, J. *Tetrahedron Lett.* **1999**, *40*, 793−796. (c) Kumar, A.; Pawar, S. S. *J. Org. Chem.* **2004**, *69*, 1419−1420.
(9) Acevedo, O.; Jorgensen, W. L.; Evanseck, J. D. *J. Chem. Theory Comput.* **2007**, *3*, 132−138.
(10) Acevedo, O. *J. Mol. Graphics Modell.* **2009**, *28*, 95−101.
(11) Sambasivarao, S. V.; Acevedo, O. *J. Chem. Theory Comput.* **2009**, *5*, 1038−1050.
(12) D'Anna, F.; Frenna, V.; Pace, V.; Noto, R. *Tetrahedron* **2006**, *62*, 1690−1698.
(13) Fontana, G.; Frenna, V.; Lamartina, L.; Natoli, M. C.; Noto, R. *J. Phys. Org. Chem.* **2002**, *15*, 108−114.
(14) Saunders, W. H., Jr. *Acc. Chem. Res.* **1976**, *9*, 19−25.
(15) Jia, Z. S.; Rudziński, J.; Paneth, P.; Thibblin, A. *J. Org. Chem.* **2002**, *67*, 177−181.
(16) Fontana, G.; Frenna, V.; Gruttadauria, M.; Natoli, M. C.; Noto, R. *J. Phys. Org. Chem.* **1998**, *11*, 54−58.
(17) Gandler, J. R.; Storer, J. W.; Ohlberg, D. A. A. *J. Am. Chem. Soc.* **1990**, *112*, 7756−7762.
(18) Gandler, J. R.; Jencks, W. P. *J. Am. Chem. Soc.* **1982**, *104*, 1937−1951.
(19) (a) Repasky, M. P.; Chandrasekhar, J.; Jorgensen, W. L. *J. Comput. Chem.* **2002**, *23*, 1601−1622. (b) Tubert-Brohman, I.; Guimarães, C. R. W.; Repasky, M. P.; Jorgensen, W. L. *J. Comput. Chem.* **2003**, *25*, 138−150.
(20) (a) Acevedo, O.; Jorgensen, W. L. *Acc. Chem. Res.* **2010**, *43*, 142−151. (b) Acevedo, O.; Jorgensen, W. L. *J. Phys. Chem. B* **2010**, *114*, 8425−8430.
(21) Acevedo, O.; Armacost, K. *J. Am. Chem. Soc.* **2010**, *132*, 1966−1975.
(22) Acevedo, O. *J. Phys. Chem. B* **2009**, *113*, 15372−15381.
(23) Sheppard, A. N.; Acevedo, O. *J. Am. Chem. Soc.* **2009**, *131*, 2530−2540.
(24) Jorgensen, W. L. *J. Phys. Chem.* **1986**, *90*, 1276−1284.
(25) Kaminski, G. A.; Jorgensen, W. L. *J. Phys. Chem. B* **1998**, *102*, 1787−1796.

(26) Thompson, J. D.; Cramer, C. J.; Truhlar, D. G. *J. Comput. Chem.* **2003**, *24*, 1291−1304.
(27) Vilseck, J. Z.; Sambasivarao, S. V.; Acevedo, O. *J. Comput. Chem.* **2011**, *32*, 2836−2842.
(28) Blagović, M. U.; Morales de Tirado, P.; Pearlman, S. A.; Jorgensen, W. L. *J. Comput. Chem.* **2004**, *25*, 1322−1332.
(29) Jorgensen, W. L.; Tirado-Rives, J. *J. Comput. Chem.* **2005**, *26*, 1689−1700.
(30) (a) Zhao, Y.; Truhlar, D. G. *Theor. Chem. Acc.* **2008**, *120*, 215−241. (b) Zhao, Y.; Truhlar, D. G. *Acc. Chem. Res.* **2008**, *41*, 157−167.
(31) Frisch, M. J. *Gaussian 09*, Revision B.01; Wallingford, CT, 2009 [Full reference given in Supporting Information].
(32) Cossi, M.; Rega, N.; Scalmani, G.; Barone, V. *J. Comput. Chem.* **2003**, *24*, 669−681.
(33) Sattelmeyer, K. W.; Tubert-Brohman, I.; Jorgensen, W. L. *J. Chem. Theory Comput.* **2006**, *2*, 413−419.
(34) (a) Dewar, M. J. S.; Yuan, Y.-C. *J. Am. Chem. Soc.* **1990**, *112*, 2088−2094. (b) Dewar, M. J. S.; Yuan, Y.-C. *J. Am. Chem. Soc.* **1990**, *112*, 2095−2105.
(35) Krop, H. B.; Cheung, C. L.; Govers, H. A. J. *J. Mol. Struct.: THEOCHEM* **2000**, *505*, 1−10.
(36) (a) Acevedo, O.; Jorgensen, W. L. *J. Chem. Theory Comput.* **2007**, *3*, 1412−1419. (b) Chandrasekhar, J.; Shariffskul, S.; Jorgensen, W. L. *J. Phys. Chem. B* **2002**, *106*, 8078−8085.
(37) Gunaydin, H.; Acevedo, O.; Jorgensen, W. L.; Houk, K. N. *J. Chem. Theory Comput.* **2007**, *3*, 1028−1035.
(38) (a) Smith, M. B.; March, J. In *March's Advanced Organic Chemistry*, 6th ed.; John Wiley & Sons: Hoboken, NJ, 2007; pp 1477−1558. (b) Reichardt, C.; Welton, T. *Solvents and Solvent Effects in Organic Chemistry*, 4th ed.; Wiley-VCH Verlag GmbH: Weinheim, Germany, 2010.
(39) An 'imaginary' frequency is a negative eigenvalue of the Hessian matrix corresponding to the motion of the system along the reaction pathway.
(40) Alunni, S.; Angelis, F. D.; Ottavi, L.; Papavasileiou, M.; Tarantelli, F. *J. Am. Chem. Soc.* **2005**, *127*, 15151−15160.
(41) (a) Amyes, T. L.; Diver, S. T.; Richard, J. P.; Rivas, F. M.; Toth, K. *J. Am. Chem. Soc.* **2004**, *126*, 4366−4374. (b) Dupont, J.; Spencer, J. *Angew. Chem., Int. Ed.* **2004**, *43*, 5296−5297.
(42) Holbrey, J. D.; Reichert, W. M.; Nieuwenhuyzen, M.; Sheppard, O.; Hardacre, C.; Rogers, R. D. *Chem. Commun.* **2003**, 476−477.
(43) Carmichael, A. J.; Seddon, K. R. *J. Phys. Org. Chem.* **2000**, *13*, 591−595.
(44) Crowhurst, L.; Mawdsley, P. R.; Perez-Arlandis, J. M.; Salter, P. A.; Welton, T. *Phys. Chem. Chem. Phys.* **2003**, *5*, 2790−2794.
(45) Deetlefs, M.; Hardacre, C.; Nieuwenhuyzen, M.; Sheppard, O.; Soper, A. K. *J. Phys. Chem. B* **2005**, *109*, 1593−1598.
(46) Jorgensen, W. L.; Severance, D. L. *J. Am. Chem. Soc.* **1990**, *112*, 4168−4114.
(47) Fu, C.-F.; Tian, S. X. *J. Chem. Theory Comput.* **2011**, *7*, 2240−2252.
(48) Takeuchi, H. *J. Phys. Chem. A* **2012**, *116*, 10172−10181.